JOURNAL OF MAGNETIC RESONANCE IMAGING 13:807–812 (2001)

Technical Note

Real-Time Black-Blood MRI Using Spatial Presaturation

Krishna S. Nayak, Ph.D.,[1]* Pedro A. Rivas, M.D.,[2] John M. Pauly, Ph.D.,[1] Greig C. Scott, Ph.D.,[1] Adam B. Kerr, Ph.D.,[1] Bob S. Hu, M.D.,[2] and Dwight G. Nishimura, Ph.D.[1]

A real-time interactive black-blood imaging system is described. Rapid blood suppression is achieved by exciting and dephasing slabs outside the imaging slice before each imaging excitation. Sharp-profiled radio frequency saturation pulses placed close to the imaging slice provide good blood suppression, even in views containing slow through-plane flow. In vivo results indicate that this technique improves endocardial border definition during systole in real-time cardiac wall-motion studies. Phantom and animal results indicate that this technique nearly eliminates flow artifacts in real-time intravascular studies. J. Magn. Reson. Imaging 2001;13:807–812. © 2001 Wiley-Liss, Inc.

Index terms: MRI; black-blood contrast; real-time imaging; pulse sequences

IN REAL-TIME IMAGING, the visualization of cardiac and vascular structures is often obscured by signal from flowing blood. For applications where flow signal and flow artifacts are obtrusive, images can be significantly improved by using "black-blood" techniques. In addition to improving endocardial border or vessel-wall definition, black-blood techniques suppress flow-related artifacts. It is a challenge to achieve good blood suppression in real time.

Currently, the most effective blood suppression techniques used in cardiovascular imaging are based on "double inversion" (1,2). Double inversion sequences suppress blood based on its flow and T_1 properties. A nonselective 180° pulse is immediately followed by a slice-selective −180° pulse; then a delay before imaging is chosen in order to null the signal from relaxing blood. Double inversion provides excellent blood suppression; however, the long inversion preparation time requires a long repetition time (TR) and is not feasible for real-time imaging.

Another technique involves using "spatial presaturation" to suppress blood (3,4). Spatial presaturation techniques suppress blood based only on flow. Immediately before each imaging excitation, a volume or volumes upstream from the slice (usually thick slabs on either side of the imaging slice) are excited and dephased. Since this technique rapidly suppresses blood, it is practical for continuous real-time imaging. This is also a steady-state technique which, for stationary objects, results in consistent signal intensity between measurements. While effective in the presence of fast through-plane flow, this technique produces reduced contrast in views containing predominantly in-plane flow (4,5). In the context of real-time imaging, spatial presaturation is a practical choice because it can be done quickly and maintains a steady state.

We present a real-time black-blood imaging sequence based on spatial presaturation. Sharp-profiled saturation pulses are used to provide good blood suppression, even in planes containing slow through-plane flow (6,7). The sequence was implemented within an existing real-time interactive imaging environment developed by Kerr et al (8). Extensions to this system include the optional volume saturation of one or two slabs before each imaging excitation, and interactive control over the saturation slab thickness, placement, and flip angle. No breathholding or gating is required. We applied this technique to real-time ventricular wall-motion study and to real-time intravascular imaging.

METHODS

Pulse Sequence

Figure 1 illustrates the basic pulse sequence. Each TR consists of spatial presaturation, which prepares the black-blood contrast, followed by an imaging acquisition. The presaturation portion (Fig. 1a) consists of two slab-selective excitations followed by a dephaser in the slice-select direction. This has the effect of nulling sig-

[1]Magnetic Resonance Systems Research Laboratory, Department of Electrical Engineering, Stanford University, Stanford, California 94305-9510.

[2]Division of Cardiovascular Medicine, Department of Medicine, Stanford University, Stanford, California 94305-5233

Grant sponsor: National Institutes of Health; Grant sponsor: GE Medical Systems; Grant sponsor: Whittaker Foundation.

Preliminary accounts of this work were presented at the Seventh Annual Scientific Meeting of the International Society for Magnetic Resonance in Medicine, Philadelphia, 1999 (abstract 1638), and the 72nd annual scientific sessions of the American Heart Association, Atlanta, 1999 (abstract 842).

*Correspondence to: Krishna S. Nayak, Packard 211, ISL, 350 Serra Mall, Stanford University, Stanford, CA 94305-9510.
E-mail: nayak@lad.stanford.edu

Received June 21, 2000; Accepted November 20, 2000.

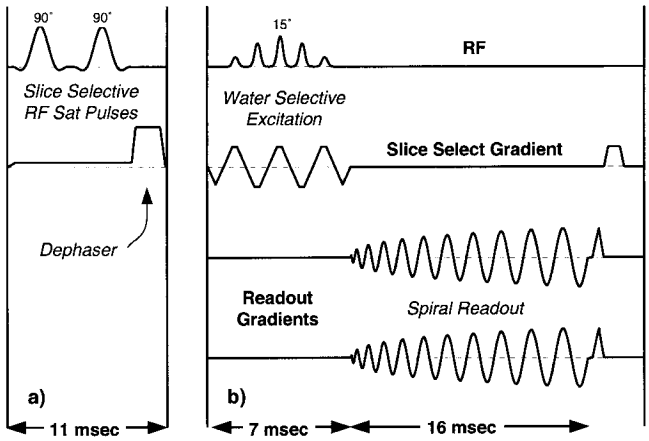

Figure 1. Real-time black–blood pulse sequence. **a:** Spatial presaturation consists of two slab-selective excitations followed by a dephaser in the slice-select direction. **b:** Imaging consists of an excitation (water-selective spectral-spatial excitation is shown), followed by imaging readouts (interleaved spirals are shown) and a gradient spoiler in the slice-select direction.

nal from the slabs, particularly the blood in the slabs which will flow into the imaging slice.

The design of sharp profiled slab excitations allows the saturated slabs to be placed close to the imaging slice for better flow suppression, without saturating spins in the imaging slice. As this technique depends on saturated blood spins flowing into the imaging slice, closer saturation slabs improve black-blood performance when through-plane flow is slow. Our slab excitations were designed using RF design tools by Pauly et al (9,10), based on the Shinnar-LeRoux technique. Simulated profiles for 2-msec and 4-msec least-squares RF saturation pulses with a design bandwidth of 2 kHz are shown in Figure 2a, illustrating how longer pulses can produce theoretically sharper slice profiles. Figure 2b contains experimentally measured profiles of these pulses obtained on a static phantom. The longer saturation pulses predictably produce a sharper profile; however, as shown by the arrow in Figure 2b (with longer pulses), the delay between the two slab excitations allows for some T_1 recovery in the first slab. One way to compensate for this is to use a flip angle slightly greater than 90° for the first slab. Another option would be to simultaneously excite both slabs with a single modulated RF pulse. This would result in the equal suppression of both slabs, but would make it difficult to adjust the slab separation and slab thickness independently and in real time.

The imaging portion of the pulse sequence (Fig. 1b) consists of a water-selective slice excitation, followed by a spiral interleaved readout and a gradient spoiler. Water-selective excitations are used to suppress signal from lipids, and interleaved spiral acquisitions provide efficient k-space coverage (11) with suppressed motion artifacts (12). While we made these excitation and readout choices for this study, the real-time interactive system supports many types of excitation (such as water-selective, slice-selective, or velocity-selective) and many k-space acquisition schemes (such as spiral, echo planar, projection reconstruction, or two-dimensional Fourier transform (2DFT).

To maintain steady state, the spatial presaturation is a part of every imaging TR, thus constituting a fixed cost of about 7–11 msec per TR. From a scan-efficiency perspective, it is therefore beneficial to use long readouts. In many cases, aggressive readout trajectories and excitations require some pulse-sequence dead time to stay within gradient duty cycle limits and amplifier heating limits. In such cases, spatial presaturation comes at a reduced cost because it does not use much gradient power and can be done during some of the dead time.

Experimental Methods

Experiments were conducted on a GE Signa 1.5 T CV/i scanner (General Electric, Inc., Milwaukee, WI). The pulse sequence was designed for gradients capable of 40 mT/m magnitude and 150 mT/m/msec slew rate, with a receiver capable of 4 μsec sampling (± 125 kHz). A body coil was used for RF transmission. For signal reception, a 5-inch surface coil was used in cardiac studies, and a custom-designed flexible twin-lead coil

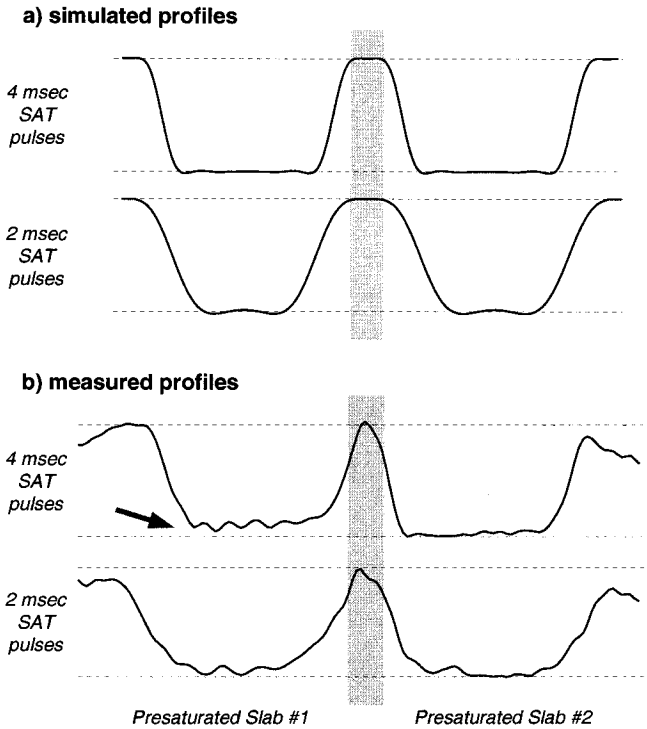

Figure 2. Simulated and measured profiles for 2-msec and 4-msec RF saturation pulses. Pulse pairs are used to saturate spins in two slabs on either side of the imaging slice. **a:** Simulations show that more precise pulses permit the saturation slabs to be placed closer to the imaging slice, potentially improving the suppression of slow through-plane flow. **b:** Measured profiles also demonstrate that 4-msec pulses allow saturation slabs to be placed closer to the imaging slice. However, using longer pulse durations creates time for T_1 recovery in the first presaturated slab (arrow). Using saturation flip angles greater than 90° for the first slab can compensate for this effect. Alternatively, the two slabs can be excited using a single modulated RF pulse.

(13,14) was used in intravascular studies. The black-blood sequence was run with a 40-msec TR. The imaging portion used 7-msec conventional spectral-spatial excitation and 16.4-msec spiral acquisitions. For cardiac studies, we used an imaging flip angle of 15°, which is the Ernst angle for myocardium (T_1 of 800 msec) at a 40-msec TR, and for intravascular studies, we used flip angles between 20–45°. The imaging slice thickness was 5–7 mm in all studies. The spatial presaturation (included in the TR) consisted of two 4-msec slab-selective excitations and a dephaser in the slice-select direction, occupying 11 msec in total. For cardiac studies, we used two-interleave spirals to achieve 2.35-mm resolution over a 20-cm field of view (FOV), at 80 msec per image. And for intravascular studies, we used six-interleave spirals for 500-μm resolution over a 2.4-cm FOV every 240 msec, or 20-interleave spirals for 360-μm resolution over a 3-cm FOV every 800 msec.

An external workstation was used to provide interactive control over scan plane and imaging parameters, and to provide real-time image reconstruction and display (8). While image acquisition was at rates of 1–12.5 images/second, a sliding window reconstruction (15) enabled display rates of up to 25 images/second.

The interactive nature of this system enabled the quick localization of standard views such as short-axis and four-chamber in cardiac studies. On the user interface, the scan plane, field of view, slice thickness, saturation band placement, and flip angle are all interactively controlled. Note that while the saturation band thickness and separation were controlled by the operator, certain default settings worked well for most cases. In cardiac short-axis views, we used a default slab thickness of 6 cm and default gap of 1.5 cm. In intravascular studies, we used a default slab thickness of 4 cm and default gap of 1.5 cm. Slab thickness and gap spacing are defined based on the profile half-maximum of slab excitations.

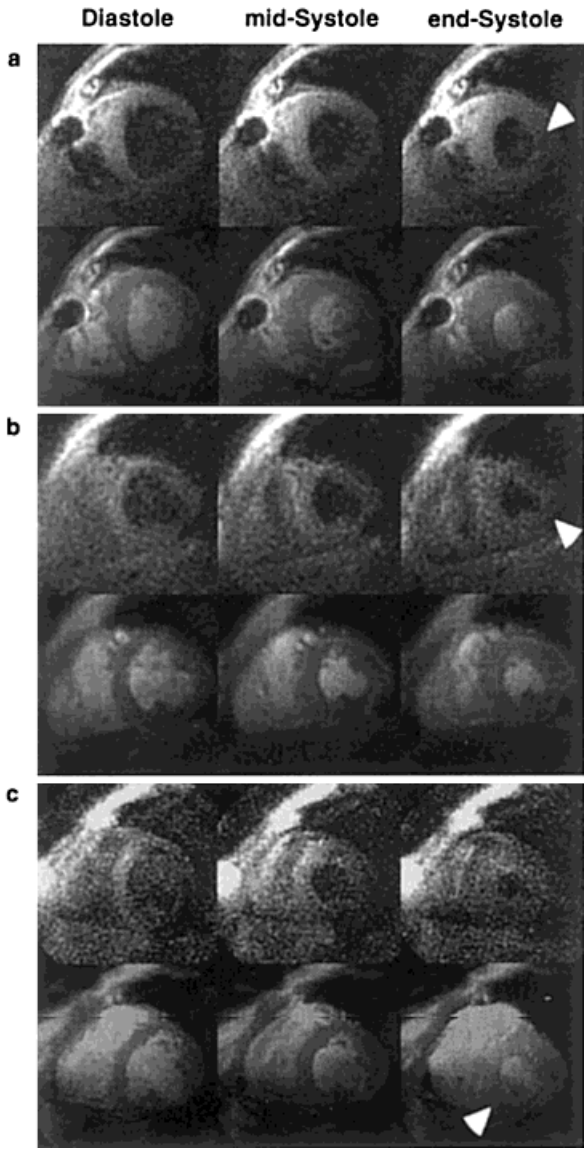

Figure 3. Short-axis comparison of black-blood and white-blood techniques during end-diastole, mid-systole, and end-systole. **a, b:** In these volunteers, arrowhead identifies improved endocardial definition at the posterior lateral LV wall. Also note the coil-sensitivity pattern. **c:** In this large volunteer, note the high noise level and signal drop-off from the large field of view. Arrowhead identifies poor white-blood contrast during systole due to significant myocardial through-plane motion.

RESULTS

We examined the utility of real-time interactive black-blood MRI in two different applications: ventricular wall-motion study and intravascular imaging.

Wall Motion

One potential application for this technique is in the evaluation of left ventricular function. Real-time white-blood techniques have proven their ability to detect wall-motion abnormalities in large patient populations (16) without gating or breathholding. In a typical real-time wall-motion study, short axis movies are acquired at various levels of the left ventricle (from apex to base), providing coverage of all relevant wall segments. In addition, the left ventricle may be segmented to accurately estimate end-diastolic and end-systolic volumes from the multiple slice data (17). One documented problem area for white-blood techniques is the often blurred blood-myocardium border during systole (16). Complex flow can present reduced blood signal, and therefore reduced contrast at the endocardial border. One way to eliminate this artifact is to employ "black-blood" techniques to image the myocardium directly, while suppressing blood and its resulting artifacts. Since short axis views involve a significant amount of through-plane flow, spatial presaturation methods may be particularly effective. Using 4-msec saturation pulses, and two-shot spiral acquisitions, we evaluated this black-blood technique in normal volunteers. Nine healthy subjects were scanned using white-blood and black-blood real-time MRI, with representative short-axis images shown in Figure 3. White-blood images were acquired with an imaging TR of 30 msec and flip angle of 30°, while black-blood images were acquired with an imaging TR of 40 msec (longer because of presaturation) and flip angle of 15°. From these images, one can

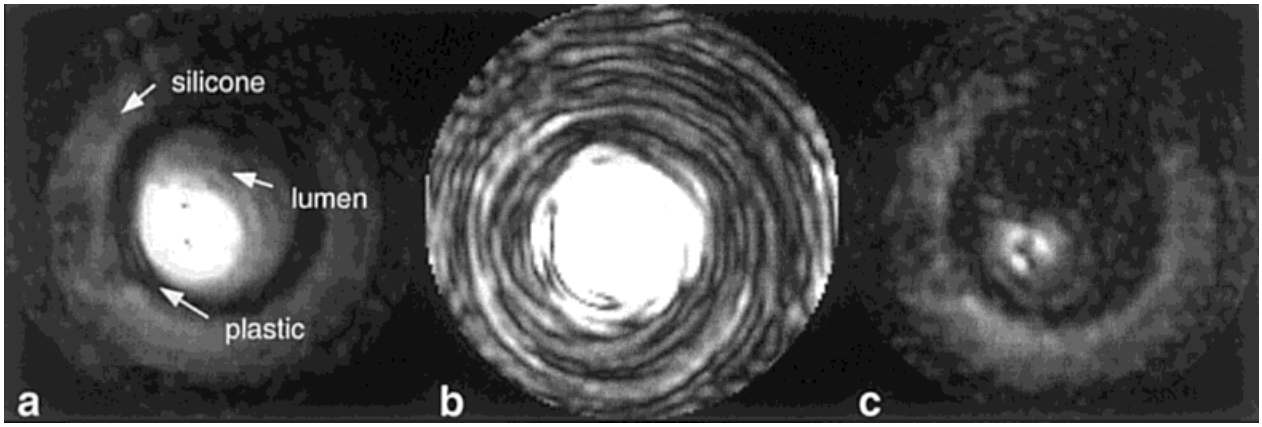

Figure 4. Intravascular flow-phantom experiment. Doped water is flowing at a constant rate through a plastic tube coated with a layer of silicone. Images were acquired (**a**) without flow, (**b**) with flow and no flow suppression, and (**c**) with water flow and flow suppression on. Relative positions of lumen, plastic tube, and silicone are identified in a. Note elimination of flow signal and flow artifacts, and preserved silicone signal in c. The remaining central signal is from fluid trapped within the coil.

observe the receiver coil sensitivity profile as well as the regional contrast improvement from using the black-blood technique. In Figure 3a,b, arrows identify improved endocardial definition around the posterior lateral wall during systole. This wall segment is particularly difficult because it moves the most and is farthest from the surface receiver coil. In Figure 3c, the arrow identifies poor white-blood contrast during systole due to significant myocardial through-plane motion. This depiction is also improved with the velocity-sensitive black-blood technique.

A contrast-to-noise ratio (CNR) analysis (18) revealed that blood-myocardium contrast in these problem areas was significantly higher in black-blood studies. CNR was calculated as

$$\frac{|S_{blood} - S_{myocardium}|}{\sigma_{noise}},$$

using regions of interest around the posterior medial wall segment, which was not biased by the coil sensitivity pattern. Problematic white-blood studies had an average blood-myocardium CNR of 1.02, while black-blood studies had an average blood-myocardium CNR of 5.27 in the same regions. In our single-coil studies, the added bias of the coil sensitivity pattern resulted in additional black-blood CNR improvements in anterior wall segments, and CNR reductions in posterior lateral segments. Other coil arrangements may be used to change this spatial variance. We also observe that while the contrast improvements can be observed in single frames (as shown in Fig. 3), the qualitative improvements are more dramatic when images are viewed in real time or in a Cine loop.

Intravascular Imaging

Intravascular imaging is another potential application for this technique. When imaging with intravascular coils, vessel/coil motion and blood flow cause significant image artifacts with prolonged scan times. For this reason, attempts have been made at real-time intravascular imaging (13). Typically in these studies, vessel cross-sectional images are acquired using an intravascular coil placed within a blood vessel. Artifacts are often disruptive to the point that vessel occlusion is necessary for wall imaging (19). By suppressing blood (which is the dominant signal in white-blood images), there may be reduced artifacts and greater signal dynamic range available for the vessel wall.

A flow-phantom experiment was performed to evaluate the quality of flow suppression which this technique could provide in a controlled setting. Real-time images were acquired using a constant-rate flow phantom. The phantom consisted of a straight plastic tube with an outside layer of silicone rubber (to provide signal). Water doped with manganese-chloride (640-msec T_1 and 90-msec T_2) was fed through the tube by a constant-rate flow pump (Masterflex model 7520-25, Cole-Parmer Instrument Co., Chicago, IL). Real-time cross-sectional images were acquired using a flexible twin-lead coil inserted within a 9-French catheter inside the phantom. Real-time images acquired using a 2.4-cm FOV and six-interleave spiral acquisitions are shown in Figure 4. The coil sensitivity pattern can be inferred from the image with no flow (Fig. 4a), which shows the relative positions of the lumen, plastic tube, and silicone outer layer. In the presence of flow, white-blood images contained significant artifacts (Fig. 4b). The strength of flow artifact signal is due both to the undisturbed M_z of flowing spins and the sensitivity of the coil being the highest near the coil center. Real-time flow suppression using spatial presaturation (Fig. 4c) resulted in the near elimination of flow signal and images containing only the static objects of interest, in this flow phantom. The only remaining central signal was from a small amount of fluid trapped within the coil.

Two rabbit experiments were then performed to evaluate the quality of blood suppression in vivo. In each experiment, a flexible twin-lead intravascular coil within a 6-French catheter was steered to the descending aorta of a sedated rabbit. Real-time vessel cross-sectional images, acquired using a 2.4-cm FOV and

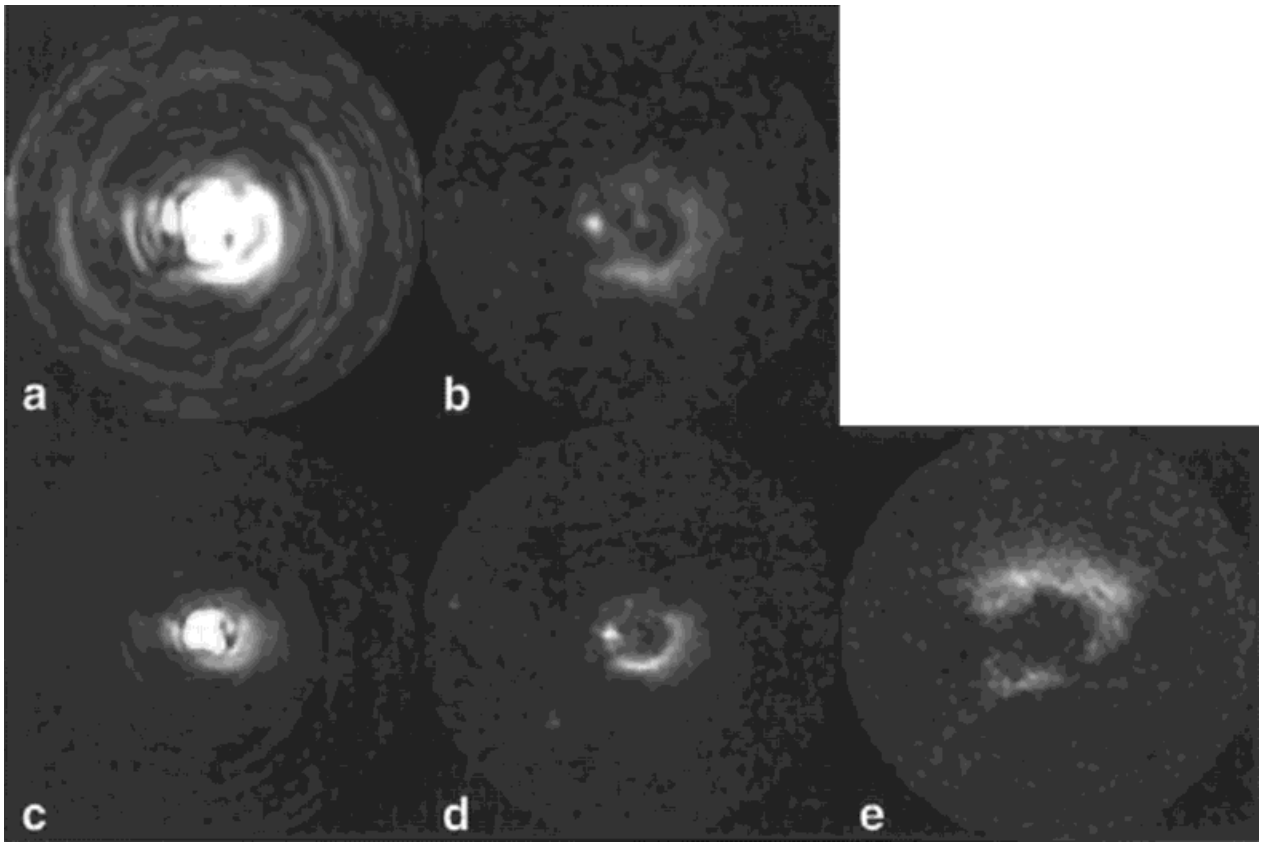

Figure 5. Intravascular coil rabbit aorta experiment. Vessel cross-section images taken with an intravascular coil in a live rabbit's descending aorta. Six-interleave images are shown (**a**) without flow suppression, and (**b**) with flow suppression. Twenty-interleave images are shown (**c**) without flow suppression, (**d**) with flow suppression, and (**e**) of lipid with flow suppression. Lipid image was acquired by setting the scan center frequency to lipids.

six-interleave spirals and using a 3.0-cm FOV and 20-interleave spirals, are shown in Figure 5. Conventional real-time images show significant artifacts due to pulsatile flow and respiratory motion (Fig. 5a,c), while flow-suppressed images of water and fat (Fig. 5b,d,e) show significantly improved wall depiction and the elimination of disruptive flow artifacts.

Note that for this application, where the region of coil sensitivity only covers one direction of through-plane flow, the sequence would be more time-efficient with just one saturation slab, placed upstream from the imaging slice.

DISCUSSION

Spatial presaturation is a practical method for acquiring black-blood images in real time. By devoting a portion of each TR to saturating out-of-slice spins, flow is suppressed and black-blood contrast is achieved, while maintaining steady-state conditions for static objects. Initial studies indicated that this technique may supplement real-time cardiac-wall motion study and improve nonoccluded intravascular imaging.

In this technique, the quality of flow suppression is directly related to the through-plane velocity component of flowing spins and to the saturation profile of suppression pulses. To be robust in the presence of slow through-plane flow, sharply profiled suppression pulses can be used at the cost of scan time (increased TR). Alternatively, if through-plane velocities are known to be large, similar black-blood contrast can be achieved with less precise saturation pulses and minimal increases in scan time.

Technical limitations of this sequence include: 1) slow flow, which may not be fully suppressed using spatial presaturation, 2) noise, which fundamentally limits real-time studies, and 3) frame rates, which are reduced because the presaturation requires additional scan time. Issues of slow flow may be addressed with improved saturation pulse design. Noise also may be addressed with the development of newer, more targeted receiver coils or coil arrays.

Real-time white-blood MRI has become a popular tool for evaluation of ventricular function, while often suffering from reduced contrast in certain segments due to flow and through-plane myocardial motion. Recently developed refocused steady state free precession (SSFP) sequences have shown improved endocardial border definition. However, rapid through-plane motion continues to degrade image contrast due to the lack of a steady state. We have demonstrated an interactive scanning system, where the ability to switch to a black-blood mode for the evaluation of these segments is beneficial. In addition, real-time black-blood MRI enables intravascular imaging in the presence of regular flow and motion, by suppressing flow and its related

artifacts. With improved resolution and suppression pulse design, applications such as real-time valve imaging (20) may also be possible.

ACKNOWLEDGMENTS

K.S.N. gratefully acknowledges the support of a Fannie and John Hertz Foundation Graduate Fellowship.

REFERENCES

1. Edelman RR, Chien D, Kim D. Fast selective black blood MR imaging. Radiology 1991;181:655–660.
2. Debbins JP, Riederer SJ, Rossman PJ, Grimm RC, Felmlee JP, Breen JF, Ehman RL. Cardiac magnetic resonance fluoroscopy. Magn Reson Med 1996;36:588–595.
3. Edelman RR, Mattle HP, Wallner B, Bajakian R, Kleefield J, Kent C, Skillman JJ, Mendel JB, Atkinson DJ. Extracranial carotid arteries: evaluation with "black blood" MR angiography. Radiology 1990; 177:45–50.
4. Felmlee J, Ehman R. Spatial presaturation: a method for suppressing flow artifacts and improving depiction of vascular anatomy in MR imaging. Radiology 1987;164:559–564.
5. Nayak KS, Pauly JM, Hu BS, Kerr AB, Nishimura DG. Real-time black-blood cardiac MRI. Circulation 1999;100:1–162. (abstract)
6. Ridgway JP, Kassner A, Sivanathan UM, Smith MA. Multiple-phase, black-blood imaging of the heart using real-time acquisition: initial results. In: Proceedings of the International Society for Magnetic Resonance in Medicine 6th Scientific Meeting, Sydney, 1998. p 807 (abstract).
7. Nayak KS, Pauly JM, Kerr AB, Nishimura DG. Real-time black-blood MRI. In: Proceedings of the International Society for Magnetic Resonance in Medicine 7th Scientific Meeting, Philadelphia, 1999. p 1638 (abstract).
8. Kerr AB, Pauly JM, Hu BS, Li KC, Hardy CJ, Meyer CH, Macovski A, Nishimura DG. Real-time interactive MRI on a conventional scanner. Magn Reson Med 1997;38:355–367.
9. Pauly JM, Roux PL, Nishimura DG, Macovski A. Parameter relations for the Shinnar-Le Roux selective excitation pulse design algorithm. IEEE Trans Med Imaging 1991;10:53–65.
10. Pauly JM, Nishimura DG, Macovski A. A linear class of large-tip-angle selective excitation pulses. J Magn Reson 1989;82:571–587.
11. Meyer CH, Hu BS, Nishimura DG, Macovski A. Fast spiral coronary artery imaging. Magn Reson Med 1992;28:202–213.
12. Nishimura DG, Irarrazabal P, Meyer CH. A velocity k-space analysis of flow effects in echo-planar and spiral imaging. Magn Reson Med 1995;33:549–556.
13. Rivas PA, McConnell MV, Nayak KS, Scott G, Meyer CH, Pauly JM, Nishimura DG, Macovski A, Hu BS. Real-time intravascular magnetic resonance receiver probe: in vivo observations in the rabbit aorta. In: Proceedings of the International Society for Magnetic Resonance in Medicine 7th Scientific Meeting, Philadelphia, 1999. p 82 (abstract).
14. Atalar E, Bottomley P, Ocali O, Correia L, Kelemen D, Lima J, Zerhouni E. High resolution intravascular MRI and MRS by using a catheter receiver coil. Magn Reson Med 1996;36:596–605.
15. Riederer SJ, Tasciyan T, Farzaneh F, Lee JN, Wright RC, Herfkens RJ. MR fluoroscopy: technical feasibility. Magn Reson Med 1988; 8:1–15.
16. Yang PC, Kerr AB, Liu AC, Liang DH, Hardy CJ, Meyer CH, Macovski A, Pauly JM, Hu BS. New real-time interactive magnetic resonance imaging complements echocardiography. J Am Coll Cardiol 1998;32:2049–2056.
17. Nagel E, Schneider U, Schalla S, Ibrahim T, Schnackenburg B, Bornstedt A, Klein C, Lehmkuhl H, Fleck E. Magnetic resonance real-time imaging for the evaluation of left ventricular function. J Cardiovasc Magn Reson 2000;2:7–14.
18. Wolfe S, Balaban R. Assessing contrast on MR images. Radiology 1997;202:25–29.
19. Martin A, Henkelman R. Intravascular MR imaging in a porcine animal model. Magn Reson Med 1994;32:224–229.
20. Arai A, Epstein F, Bove K, Wolff S. Visualization of aortic valve leaflets using black blood MRI. J Magn Reson Imaging 1999;10: 771–777.